Electromagnetic force on structured metallic surfaces

Andrew H. Velzen and Kevin J. Webb

The Electromagnetic Force on Structured Metallic Surfaces

Andrew H. Velzen and Kevin J. Webb

Purdue University

465 Northwestern Avenue,

West Lafayette, Indiana 47907-1285, USA

webb@purdue.edu

Abstract

We present a method by which the relatively weak electromagnetic force exerted on a surface can be dramatically enhanced. By structuring a metal surface at the nanoscale, we show that the force can be substantially increased over that on the planar metallic surface. The basis for this effect is found to be cavity-enhanced fields and the excitation of surface waves, and results are related to theory. In practice, this force enhancement could be expanded to other materials in various frequency regimes. This larger sensitivity to electromagnetic force should facilitate an expansion of applications related to optomechanics.

PACS numbers: 78.68.+m; 78.67.-n; 78.20.-e; 78.70.-g; 45.20.da

The radiation pressure on a mirror was measured more than one century ago[1], and subsequent experiments have yielded more information[2]. Other experiments have shown traps that result from a spatially varying electromagnetic field that influence polarizable media[3,4], which is the basis of laser tweezers[3]. More generally, electromagnetic forces in micro-scale systems have produced an array of possible applications[5], and resulted in the field of optomechanics[6,7]. In pursuing applications related to the mechanical response of structured material to incident electromagnetic radiation, the description of the force density on that length scale is required (see, for example,[8]).

The fact that electromagnetic fields, created by charges, can instantiate a force on other charged particles has been known since the time of Coulomb. Lorentz mathematically described the force on an electron in vacuum as $\mathbf{F} = q\mathbf{E} + q\mathbf{v} \times \mu_0 \mathbf{H}$, where $\mathbf{E}$ is the electric field, $\mathbf{H}$ is the magnetic field, q is the charge (on the electron), $\mathbf{v}$ is the instantaneous velocity, and μ_0 is the free space permeability (and SI units are implied)[9].

The description of the electromagnetic force density has been presented by Einstein and Laub[10] and others[11–16]. This theory has two terms associated with the force that are consistent with experiments. The radiation pressure on the medium[11] arises from the flow of energy associated with the electromagnetic field's Poynting vector[2]. The spatially varying field produces a divergence term[11] that results in a lensing effect when a laser illuminates a liquid[17]. While there has been some debate as to how to describe electromagnetic momentum in the context of the formation of a force expression, experiments have elucidated pressure and spatial field variation components that are captured by Einstein and Laub[10,18] and are consistent with a coupled system picture[11].

Our analysis herein demonstrates that by structuring the surface of a metal, one can achieve a larger, and in some cases considerably larger, electromagnetic force acting on the metallic sample than is possible without the nanostructure. We consider cavities in a gold (Au) surface, as in Fig. 1(a), and the sawtooth structure of Fig. 1(b). A planar metal film illuminated by a normal plane wave experiences only a radiation pressure component of the force. By structuring the surface of the metal, the spatial variation of the fields inside the metal and near to the surface result in an additional and much larger force component in the same direction as the radiation pressure. Consequently, it becomes possible to increase the sensitivity of mechanical actuation using electromagnetic forces from, for example, a laser. The enlarged force could intensify the cavity response of induced optomechanical

oscillators[6], enhance optical cooling of micromechanical oscillators and micromirrors[19,20], allow for greater control of photonic/optomechanical devices[7,21,22], and produce greater sensitivity in sensors utilizing optomechanical oscillation[23].

We utilize a force description that we have discussed in our previous work[24–27] that has been developed by Penfield and Haus[11] and is consistent with the Einstein and Laub form[10]. Using this description, the electromagnetic kinetic force density in material media becomes

$$\mathbf{f} = \frac{\partial \mathbf{P}}{\partial t} \times \mu_0 \mathbf{H} - \frac{\partial \mu_0 \mathbf{M}}{\partial t} \times \epsilon_0 \mathbf{E} + \rho \mathbf{E}$$
$$- \mu_0 \mathbf{H} \times \mathbf{J} + (\mathbf{P} \cdot \nabla)\mathbf{E} + \mu_0 (\mathbf{M} \cdot \nabla)\mathbf{H}, \tag{1}$$

with $\mathbf{f}$ having SI units of N/m^3 and $\mathbf{P}$ the polarization, $\mathbf{M}$ the magnetization, $\mathbf{J}$ the free electric current density, ρ the free electric charge density, and ϵ_0 the permittivity of free space. In our special case, the free current and free charge densities will both be zero, and we also assume there is no magnetic material response, so the terms involving $\mathbf{M}$ in (1) are zero. Consequently, one term in (1) describes the radiation pressure, $\partial \mathbf{P}/\partial t \times \mu_0 \mathbf{H}$, and one the gradient force, $(\mathbf{P} \cdot \nabla)\mathbf{E}$. Our interest here is the force that can be exerted on a structured metal surface by laser light, and from (1), the force density within the metal becomes

$$\mathbf{f} = \frac{\partial \mathbf{P}}{\partial t} \times \mu_0 \mathbf{H} + (\mathbf{P} \cdot \nabla)\mathbf{E}. \tag{2}$$

We consider a time-harmonic, monochromatic field with frequency dependence $\exp(-i\omega t)$ and an isotropic dielectric response, giving $\mathbf{P}(\mathbf{r}, \omega) = \epsilon_0 \chi_E(\mathbf{r}, \omega)\mathbf{E}(\mathbf{r}, \omega)$, with χ_E the electric susceptibility (and dielectric constant $\epsilon = 1 + \chi_E$). With the frequency domain implied, the polarization can then be written as

$$\mathbf{P}(\mathbf{r}, t) = \hat{\mathbf{e}} \frac{\epsilon_0}{2\pi} [\chi_E(\mathbf{r})E(\mathbf{r})e^{-i\omega t} + \text{c.c.}], \tag{3}$$

where $\hat{\mathbf{e}}$ is a unit vector, E is the phasor electric field, and c.c. represents the complex conjugate of the first term inside the brackets. By defining $\mathbf{E}$ and $\mathbf{H}$ similarly, the time average of the force density in (2) becomes

$$\langle \mathbf{f} \rangle = (\hat{\mathbf{e}} \times \hat{\mathbf{h}}) \frac{\mu_0 \epsilon_0 \omega}{2\pi^2} \Im\{\chi_E E(\mathbf{r}) H^*(\mathbf{r})\}$$
$$+ \frac{\epsilon_0}{2\pi^2} \Re\{(\chi_E E(\mathbf{r}) \, \hat{\mathbf{e}} \cdot \nabla)(\hat{\mathbf{e}} E^*(\mathbf{r}))\}, \tag{4}$$

where $\Re\{\cdot\}$ is the real part and $\Im\{\cdot\}$ is the imaginary part. Following a numerical solution for the fields, we use (4) to obtain the time-averaged force density, and then form the pressure

3

by integrating the $y-$component of the force density over the depth of the structure as $\langle p_y \rangle = P^{-1} \int \langle f_y \rangle dx dy$, using the example of Fig. 1(a) where the period in the x-direction is P, with units of N/m^2.

Consider the two structured Au metal films in Fig. 1 with free space above and below. A 2D numerical finite element method solution[28] for the fields used periodic boundary conditions on the left and right and assumed a plane wave normally incident from above with E_x, H_z (note the coordinate system in the lower left of each figure). The top and bottom surfaces of the simulation domain were implemented as port boundaries so that the scattered waves are absorbed to simulate semi-infinite domains. A wavelength of 633 nm was used and the complex dielectric constant for Au was taken from the literature[29]. We studied the arrangement of Fig. 1(a) with 30 nm and 60 nm wide slots of varying depths, as well as the sawtooth geometry of Fig. 1(b). With the polarization considered, plasmonic cavity modes can form in the slot[30]. We analyzed a number of structures to evaluate the influence of a nanostructured surface on the optical force experienced by the sample. In order to consider a situation representative of an experiment, the Poynting vector of the incident plane wave was normalized for an illumination power density equivalent to 1 mW over a uniformly illuminated circular spot size of diameter 1 μm.

For the slot geometry of Fig. 1(a), we solved for the fields for slot widths (W) of 30 nm and 60 nm, and depths (D) ranging from 1 nm to 90 nm, in steps of 1 nm. Field plots for three slot depths for the 60 nm wide slot are given in Fig. 2. Note that as the slot depth is increased, the cavity passes through a resonance (as measured by the integral of the magnitude of the field in the cavity), the case of Figs. 2(c) and (d). We calculated the average force density from (4) using the numerical solutions for the fields, and upon integration over the thickness of the film, found the pressure on the Au film, $\langle p_y \rangle$. Plots of the $y-$component of force density, $\langle f_y \rangle$, are given in Fig. 3 for a 30 nm wide slot and slot depths of 1, 51, and 81 nm. Notice that the force distribution varies considerably as a function of slot depth.

The field solutions and $y-$component of force density for the sawtooth structure of Fig. 1(b) are shown in Fig. 4. While the force density is large near the vertices in the Au, the net force is not as large as can be achieved with the resonant slot structure, where a resonance can be excited with the normally incident field. However, the pressure on the sawtooth is still higher than results from a planar Au film. For comparison, Table I gives

4

macroscopic pressures for each nanostructured surface. While the sawtooth produced a slightly higher pressure, the Au film with slots at resonance resulted in a dramatic increase in the pressure. With the narrower slot a higher quality factor resonance results, and the concomitant increase in the field strength in the cavity produces an increased pressure. Note that the fields can have rapid spatial variations that impact both the magnitude and the sign of the local force density, as illustrated in Fig. 3 and Fig. 4(c).

In order to develop a better picture of the relative force enhancement as a function of slot geometry, Fig. 5 gives the pressure, $\langle p_y \rangle$, for the 30 nm and 60 nm slot widths as a function of slot depth with a (normalized) input power density of 1 W/m^2. The maximum pressure occurs at the resonant depth, and the peak pressure is higher for the 30 nm slot case.

Consider the simple approximation where the planar Au surface is treated as a perfect electric conductor (PEC), which assumes that the imaginary part of the dielectric constant approaches plus infinity or, equivalently, that the real part approaches minus infinity. Consequently, the skin depth goes to zero and the total field in the incident half-space has zero tangential electric field and a maximum in the magnetic field. The radiation pressure on this surface becomes[18]

$$\langle p_y \rangle = \frac{4 S_{-y} k}{\omega} = \frac{4 S_{-y}}{c}, \tag{5}$$

where S_{-y} is the incident power density (Poynting vector magnitude in the $-y$-direction), k is the (free space, in this case) wave number, and c is the speed of light in vacuum. Normalizing to $S_{-y} = 1$ W/m^2, we find an analytical macroscopic pressure of 1.33×10^{-8} N/m^2 on the PEC. The value we found through simulation for a planar Au (with $\epsilon = -11.82 + i1.23$) surface was 1.29×10^{-8} N/m^2, which is the zero slot depth result in Fig. 5.

To ascertain the primary mechanism by which this force enhancement occurs, consider a decomposition of the pressure into two components, one corresponding to the radiation pressure term, or cross term, in (2) and the other to the diverging electric field term, or divergence term. Figure 6 shows the numerical results of this decomposition. Far from resonance, the term associated with radiation pressure dominates (for cavity depths less than about 35 nm and greater than 90 nm). This is because there is relatively little spatial variation of the field. As can be seen in Fig. 3(a), where the surface is almost perfectly planar, the force density is significant within about one skin depth of the surface. As resonance is approached, the magnitude of the fields in the cavity increase, as does the spatial variation of the field, leading to an increase in the divergence term, as in Fig. 3(b). At resonance,

the divergence component dominates, and is thus primarily responsible for the significant force enhancement. Further analysis of Fig. 3(b) shows an enhancement of the force density near the top surface when the slot is resonant. We interpret this to be due to the more efficient excitation of the surface wave on the top surface of the metal film when the cavity is resonant, and that this surface wave contributes to the pressure on the film, thus yielding an increase in the cross term as well. The periodic boundary condition on the left and right of the computation domain results in a standing surface wave, and this is evident in Fig. 2(f).

By conservation of momentum, the greatest momentum an electromagnetic wave could impart is twice the incident momentum, which would happen in the case of total reflection. This momentum exchange has been measured to depend of the refractive index of the background[31]. The kinetic force density, as described by (1), depends on both the spatial variation of the fields and the homogenized material parameters. As we have demonstrated, it is possible to substantially enhance the total force through control of the nanostructure. It should be noted that this does not inherently violate conservation of momentum, as momentum and force are interrelated, but distinct. It is presumably also possible to further control the force through the material properties, the sign of the real part of the dielectric constant (metal or dielectric), and the imaginary part (loss or gain[25]). Also, one could potentially use magnetic materials to further enhance the force density, thereby including the two magnetization terms in (1) that we disregarded.

The pressure on the walls of a cavity results from, and can be modified by, excitation of the cavity mode, and the increase in force on one of two metal plates has been shown to increase at the resonant wavelength[32]. In contrast, we have shown that the total pressure on a contiguous metal film can be increased over the planar case, which is quite distinct. In the cited work, the roughness is found to increase the magnitude of the pressure at resonance and to make it more negative on the back mirror (with the positive direction being that of the incident Poynting vector). In the situations we consider, the roughness increases the pressure (makes it more positive) with respect to the flat film in all cases. We find it interesting that in our work, nanostructuring resulted in an increase in pressure, while earlier work related to the Casimir force found the structuring of a metallic surface reduced that force[33].

It is certainly possible to build such a nanostructured surface, as in Fig. 1, through meth-

ods like resistless nanoimprint into metal[34] or focused ion beam milling. This could allow one to not only experimentally verify our results, but utilize them in significant applications as well. One example would be for use in optomechanical wavelength routing. By placing nanostructures on the surface of ring resonators[22], it should be possible to achieve a greater force or a reduced switching time. Such a switching arrangement could lead to more energy efficient routing of optical signals. The nanostructured force enhancement technique we present could also be used to enhance the optomechanical properties of a Fabry-Pérot interferometer. Radiation pressure has been used to cool a cavity by counter-acting the motion of one mirror[20,35]. These cavities are important in fundamental quantum mechanical and gravitational wave experiments. If one were to modify the mirror in some meaningful way to achieve greater sensitivity to the optical force, it should be possible to improve the performance through a reduction in the optical control signal power or by reducing the response time and hence achieving a lower cavity temperature.

In all cases studied, structuring the metallic surface provides at least some increase in the force experienced by the metal surface. The case of the resonant 30 nm slot in Au at 633 nm resulted in approximately a 23-fold enhancement. This leads to the position that metallic surfaces with roughness can experience greater electromagnetic force than those without surface roughness. Presumably, pressure could be increased by increasing the density of the nanoslots in the metal film. We also anticipate that other structured materials, such as dielectrics, will similarly increase the pressure. In the case of the Au film studied, the resonant slot produces both a larger cavity field and an efficient means to excite the surface plasmon, and both contribute to the pressure enhancement. Finally, our treatment was based on (2). We expect that other relevant models will have a cross term (the standard radiation pressure) and a divergence term (that is used in optical tweezers), and that similar effects will result, but possibly with differing quantitative conclusions on the enhancement. Experiments motivated by this work could have the goal of verifying the relevant modeling issues.

------

[1] E. Nichols and G. Hull, Phys. Rev. (Series I) **17**, 26 (1903).

[2] R. V. Jones and B. Leslie, Proc. Royal Soc. A **360**, 347 (1978).

[3] A. Ashkin, J. M. Dziedzic, J. E. Bjorkholm, and S. Chu, Opt. Lett. **11**, 288 (1986).

[4] D. G. Grier, Nature **424**, 810 (2003).

[5] A. W. Rodriguez, P. Hui, D. P. Woolf, S. G. Johnson, M. Lončar, and F. Capasso, Ann. Phys. **527**, 45 (2015).

[6] T. J. Kippenberg, H. Rokhsari, T. Carmon, A. Scherer, and K. J. Vahala, Phys. Rev. Lett. **95**, 033901 (2005).

[7] D. Van Thourhout and J. Roels, Nature Photon. **4**, 211 (2010).

[8] M. I. Antonoyiannakis and J. B. Pendry, Phys. Rev. B **60**, 2363 (1999).

[9] H. A. Lorentz, *The Theory of Electrons*, vol. 29 (BG Teubner, 1916).

[10] A. Einstein and J. Laub, Ann. Phys. **331**, 541 (1908).

[11] P. Penfield and H. A. Haus, *Electrodynamics of Moving Media* (MIT Press, Cambridge, MA, 1967).

[12] L. J. Chu, H. A. Haus, and P. Penfield, Proc. IEEE **54**, 920 (1966).

[13] J. P. Gordon, Phys. Rev. A **8**, 14 (1973).

[14] I. Brevik, Phys. Rep. **52**, 133 (1979).

[15] I. Brevik, arXiv preprint arXiv:1310.3684 (2013).

[16] M. Mansuripur, Opt. Comm. **283**, 1997 (2010).

[17] A. Ashkin and J. M. Dziedzic, Phys. Rev. Lett. **38**, 1351 (1977).

[18] K. J. Webb, Phys. Rev. Lett. **111**, 043602 (2013).

[19] S. Gigan, H. Böhm, M. Paternostro, F. Blaser, G. Langer, J. Hertzberg, K. Schwab, D. Bäuerle, M. Aspelmeyer, and A. Zeilinger, Nature **444**, 67 (2006).

[20] A. Schliesser, P. DelHaye, N. Nooshi, K. J. Vahala, and T. J. Kippenberg, Phys. Rev. Lett. **97**, 243905 (2006).

[21] G. S. Wiederhecker, L. Chen, A. Gondarenko, and M. Lipson, Nature **462**, 633 (2009).

[22] J. Rosenberg, Q. Lin, and O. Painter, Nature Photon. **3**, 478 (2009).

[23] Y. Deng, F. Liu, Z. C. Leseman, and M. Hossein-Zadeh, Opt. Expr. **21**, 4653 (2013).

[24] Shivanand and K. J. Webb, J. Opt. Soc. Am. B **29**, 3330 (2012).

[25] K. J. Webb and Shivanand, Phys. Rev. E **84**, 057602 (2011).

[26] K. J. Webb and Shivanand, J. Opt. Soc. Am. B **27**, 1215 (2010).

[27] K. J. Webb and Shivanand, J. Opt. Soc. Am. B **29**, 1904 (2012).

[28] *COMSOL Multiphysics*, http://www.comsol.com/comsol-multiphysics.

[29] P. B. Johnson and R. W. Christy, Phys. Rev. B **6**, 4370 (1972).

[30] K. J. Webb and J. Li, Phys. Rev. B **73**, 073404 (2006).

[31] G. K. Campbell, A. E. Leanhardt, J. Mun, M. Boyd, E. W. Streed, W. Ketterle, and D. E. Pritchard, Phys. Rev. Lett. **94**, 170403 (2005).

[32] S. B. Wang, J. Ng, H. Liu, H. H. Zheng, Z. H. Hang, and C. T. Chan, Phys. Rev. B **84**, 075114 (2011).

[33] F. Intravaia1, S. Koev, I. W. Jung, A. A. Talin, P. S. Davids, R. S. Decca, V. A. Aksyuk, D. A. R. Dalvit, and D. López, Nat. Comm. **4:2515** (2013).

[34] S. Kim, Y. Xuan, V. P. Drachev, L. Y. Varghese, L. Fan, M. Qi, and K. J. Webb, Opt. Expr. **21**, 15081 (2013).

[35] D. Kleckner and D. Bouwmeester, Nature **444**, 75 (2006).
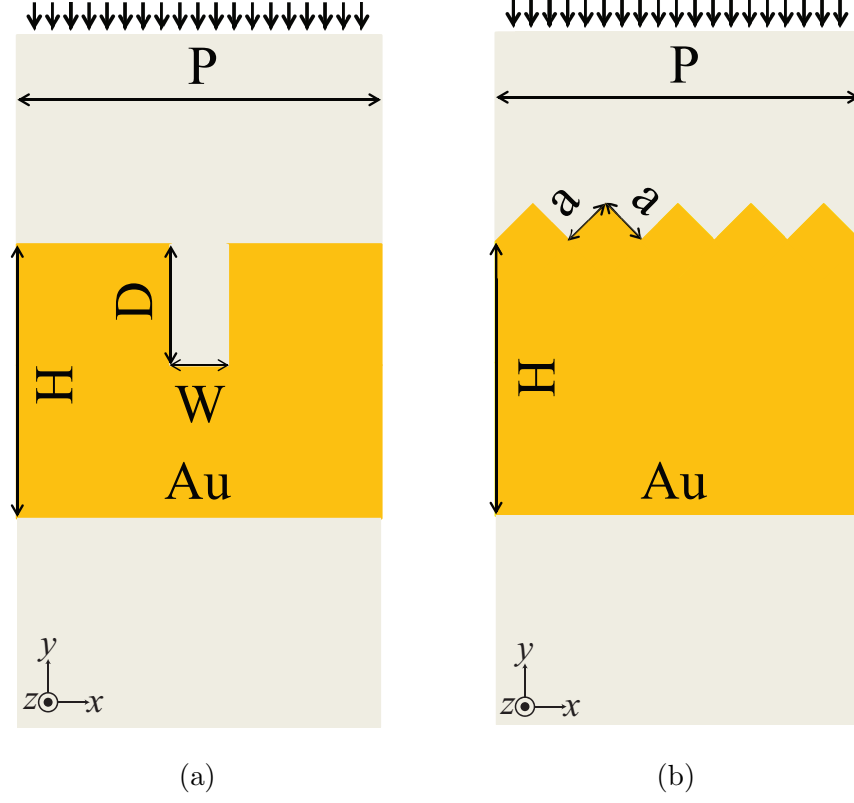
Figures

FIG. 1: Simulated gold (Au) metal film structures in free space: (a) slot and (b) sawtooth. For (a), D is varied between 1 nm and 90 nm, with W set to 30 nm and 60 nm. For (b), a is 56 nm. In all cases, the Au sample is illuminated from the top by 633 nm light (E_x, H_z), P is 400 nm, H is 200 nm. Periodic boundary conditions are enforced on the left and right, are port boundaries are on the top and bottom.
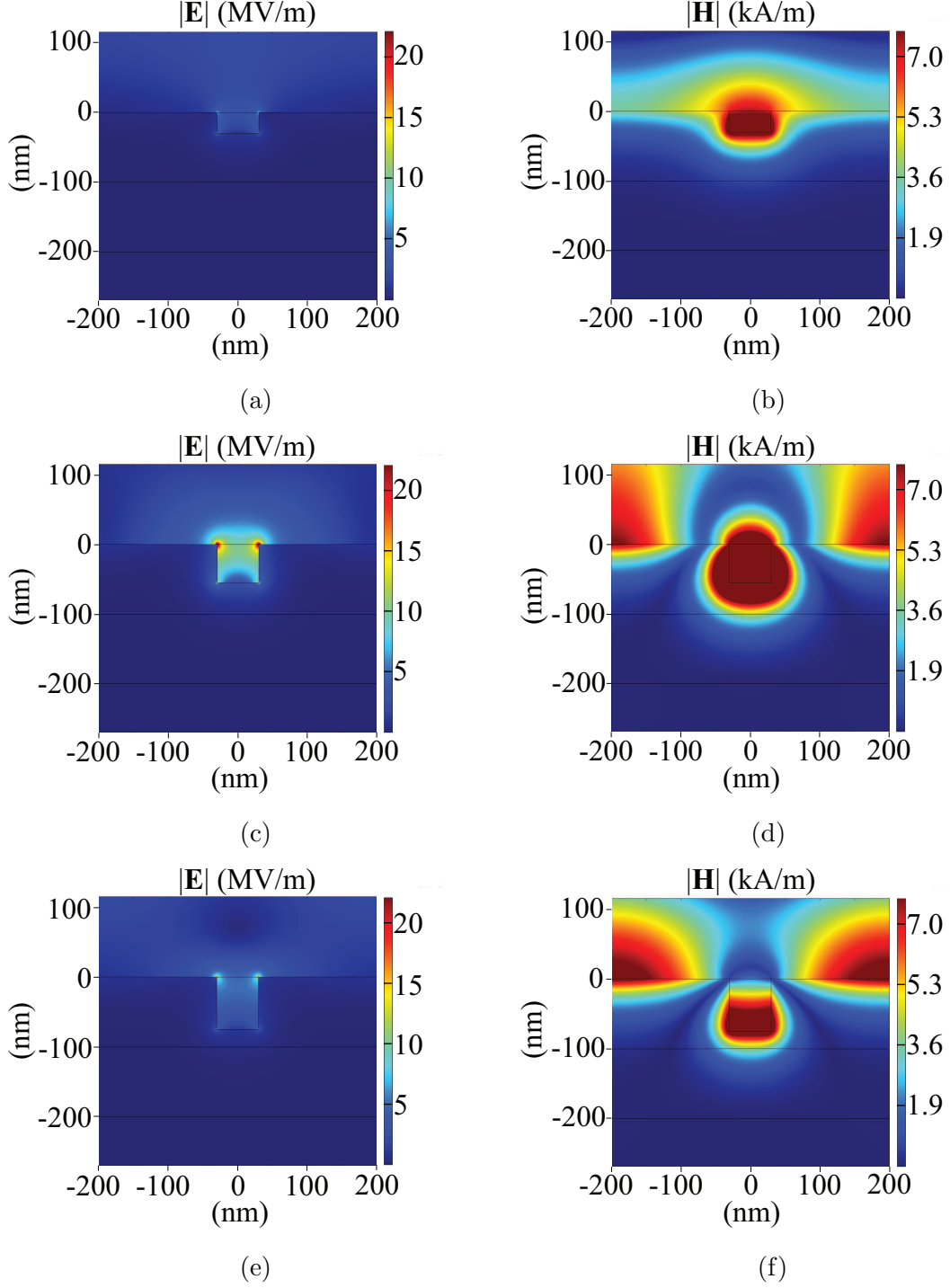
FIG. 2: **E** and **H** magnitudes for the 60 nm slot width for slots depths of: (a) and (b) 30 nm; (c) and (d) 55 nm; and (e) and (f) 75 nm. The power density of the incident Poynting vector is normalized to 1 mW with 633 nm laser illumination over a circular spot size of diameter 1 μm. For reference, resonance is achieved at 55 nm.
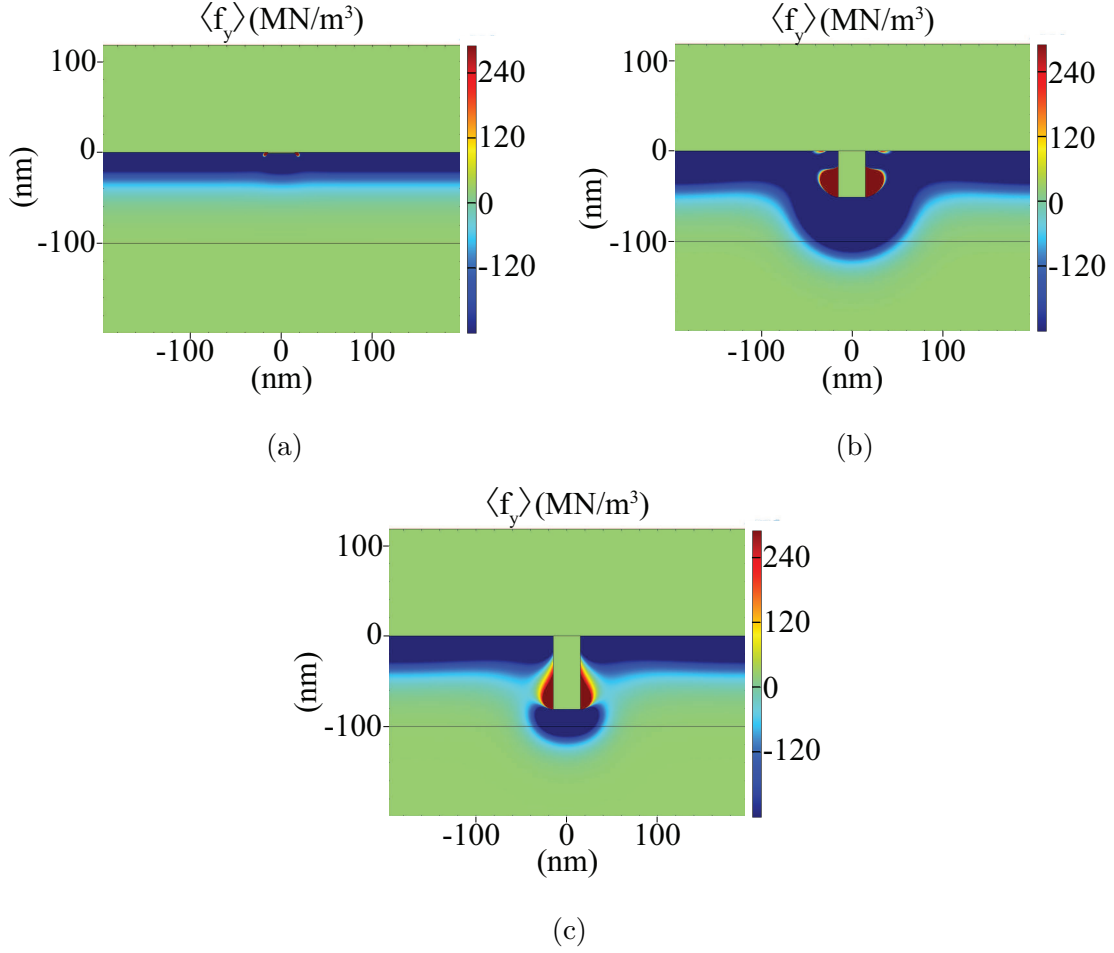
FIG. 3: The $y-$component of the force density for the 30 nm wide slot at various slot depths: (a) 1 nm; (b) 51 nm: (c) 81 nm. The simulation has an incident power density equivalent to 1 mW of 633 nm laser illumination over a circular spot of diameter 1 μm. For reference, resonance is achieved at about 46 nm for the 30 nm wide slot.
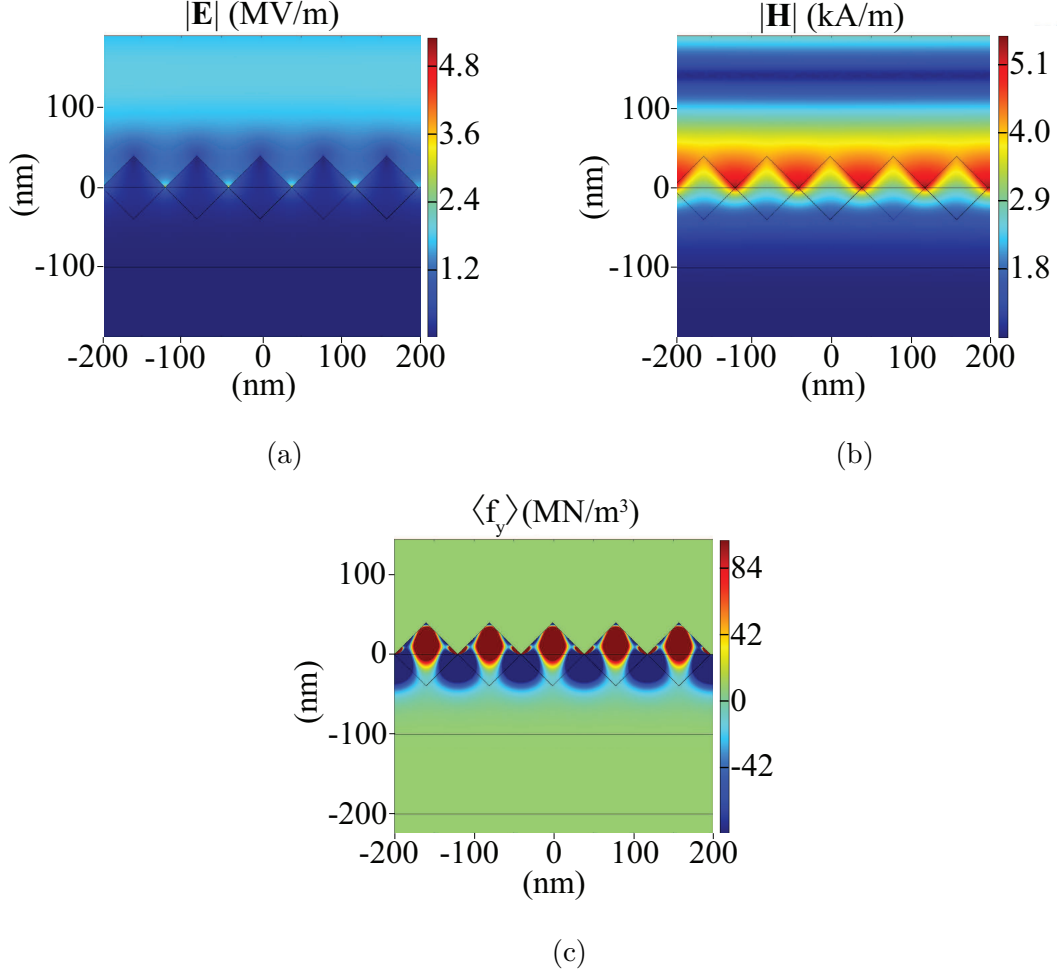
|E| (MV/m)

(a)

|H| (kA/m)

(b)

⟨f_y⟩(MN/m³)

(c)

FIG. 4: Sawtooth geometry results. (a), (b), and (c) represent the magnitude of **E**, magnitude of **H**, and $y-$component of the force density for the sawtooth geometry, respectively. The simulation has an incident power density equivalent to 1 mW of 633 nm laser illumination over a circular spot of diameter 1 μm.
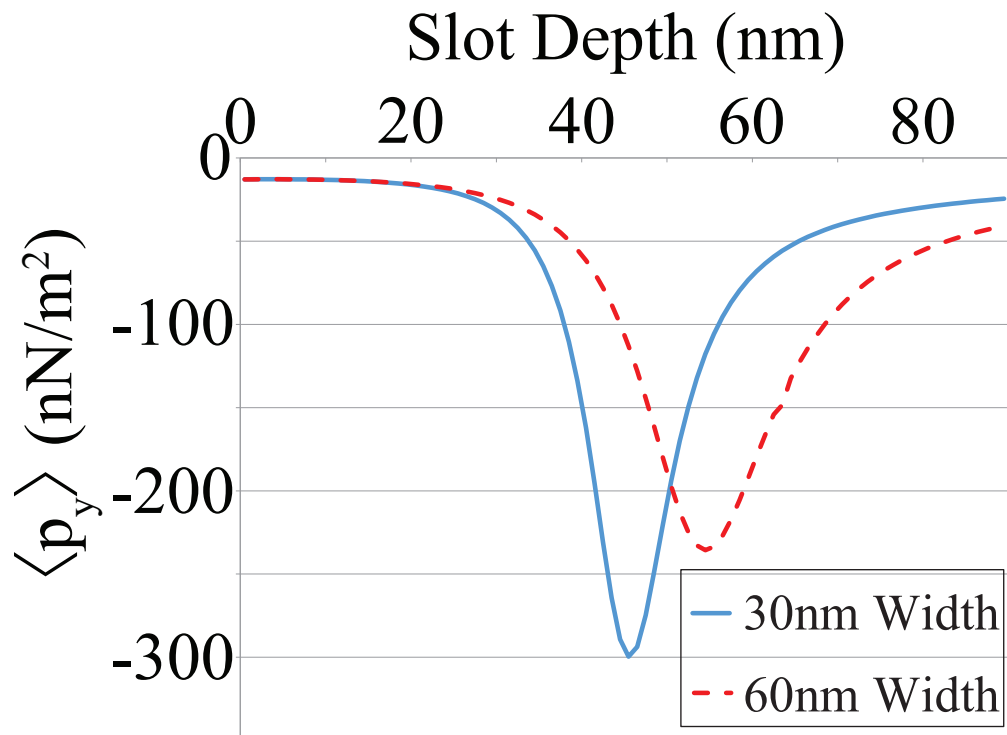
FIG. 5: Numerical results for the pressure as a function of slot depth in a Au film for the two slot widths, calculated for slot depths from 1 nm to 90 nm in 1 nm steps and $\langle p_y \rangle$, in N/m^2, determined by integrating the $y-$component of force density over the depth of the Au nanostructure. These values are normalized to a Poynting vector power density of 1 W/m^2 and the wavelength is 633 nm.
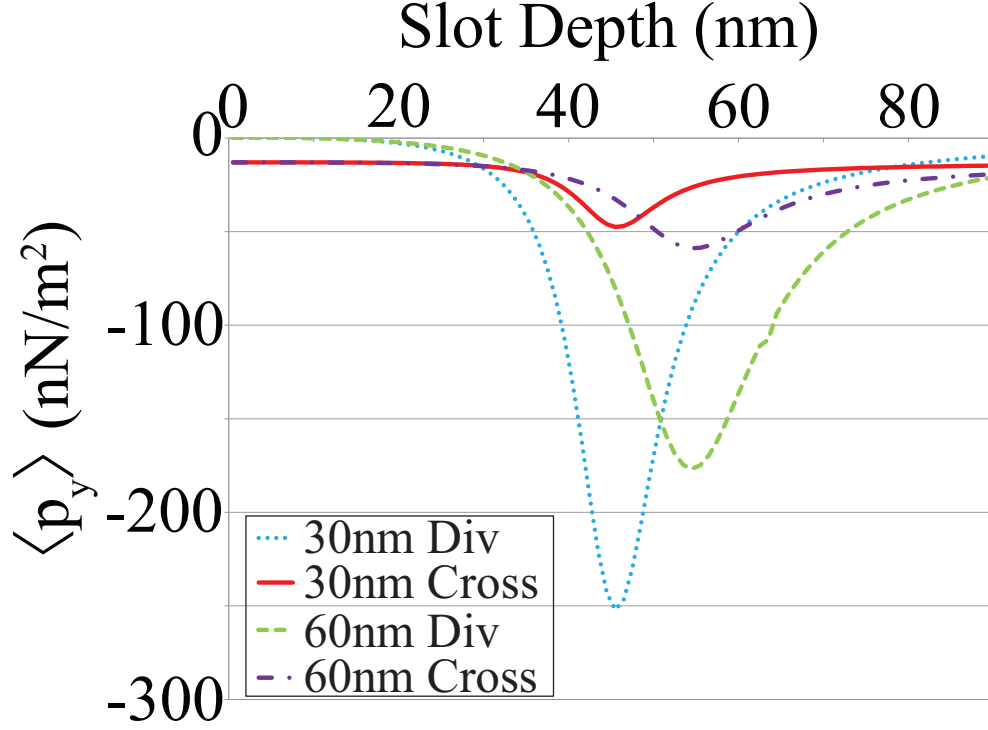
FIG. 6: Magnitude of the two force terms with the force density calculated at slot depths from 1 nm to 90 nm in steps of 1 nm for the 30 nm and 60 nm wide slots. The force density is separated into one component due to the $(\nabla \cdot \mathbf{P})\mathbf{E}$ term, which we call the divergence term, and another due to the $\mu_0 \mathbf{H} \times \partial \mathbf{P}/\partial t$ term, which we call the cross term. The $y-$component of the force density is separately integrated over the depth of the Au nanostructure for each term, divergence and cross. This yields a pressure in $\mathrm{N/m}^2$. These values are normalized to a Poynting vector power density of 1 $\mathrm{W/m}^2$ of 633 nm laser illumination.

Tables

Various Nanostructured Gold Pressure Values	
Nanostructure	$\langle p_y \rangle$ **in N/m^2**
Planar surface	-1.29×10^{-8}
56 nm square sawtooth	-1.77×10^{-8}
Resonant 60 nm slot	-2.36×10^{-7}
Resonant 30 nm slot	-3.00×10^{-7}

TABLE I: Comparison of calculated pressures on a planar Au surface, the sawtooth structured surface, and two difference examples of plasmonic cavities formed by slots in the Au surface. These results are for an incident power density equivalent to 1 mW of 633 nm laser illumination over a circular spot of diameter 1 μm.